Geological Survey of Japan Cruise Report No. 18, p. 36–45, 1982

II. MAGNETIC AND GRAVITY PROFILES OF THE WAKE-TAHITI TRANSECT, GH80-1 CRUISE

Masato Joshima and Yoshihisa Okuda

We conducted a geomagnetic survey and a gravity measurement in GH80–1 cruise with a Marine Proton Magnetometer (Geometrix Model G801) and a gyrostabilized La Coste and Romberg Sea Air Gravity Meter S-63, respectively. Almost continuous data were obtained on the two survey lines, A and B (see Chapter I), except for their some parts due to leaking of sea waters into sensor and malfunction of the magnetometer (for magnetic data) and breaking down of gyro in platform of the gravity meter (for gravity data).

The magnetic and gravity anomaly profiles obtained through calculations of raw data are shown in Fig. II-1 (compiled for the entire survey lines) and Fig. II-2 (detailed for every intervals of sampling stations on the lines).

Magnetic data

Magnetic anomaly was calculated by subtracting IGRF (International Geomagnetic Reference Field, 1975) from measured total magnetic intensity. We can recognize several intervals with fairly strong anomaly (p-p 200 nT) and wave lengths of 10 to 20 km.

The anomaly pattern, rather regular, between Sts. 1593 and 1594 on Line A and between Sts. 1638 and 1642 on Line B can be interpreted to be M11-M9-M11 Magellan lineations which are characterized by fan-shaped symmetric anomaly sequence (TAMAKI *et al.*, 1980). The Phoenix lineations in the equatorial Pacific (LARSON *et al.*, 1972; LARSON, 1976) seems to be partly represented by the pattern of Sts. 1599 to 1601 on Line A, though a precise identification is difficult due to the missing of data on the expected part of the lineations south of St. 1601. On Line B, we can recognize marked anomalies with a wave length of about 30 km between Sts. 1634 and 1635, but to the south magnetic anomalies become very irregular and broad. Also, magnetic anomalies on both sides of the Nova-Canton Trough (ROSENDAHL, 1975) can not be well characterized by our data. The Sts. 1634–1635 anomalies may be possibly identified to any sequence of the Phoenix lineations. It is noted, however, that further detailed study is necessary regarding this problem, because the areas around the stations and of their northward occupy the junction zone of the Phoenix (on the south), Magellan (on the north), and the Central Pacific lineations (on the east; OEWIG and KROENKE, 1980), and more detailed data may help better understanding of the Mesozoic development of the Central Pacific Basin.

Although our data are insufficient, magnetic anomalies in the Penrhyn Basin seem to be characterized by small amplitude and short wave length, possibly implying the origin of the basin during the magnetic quiet zone in the late Cretaceous as postulated by WINTERER *et al.* (1974) from a bathymetric point of view.

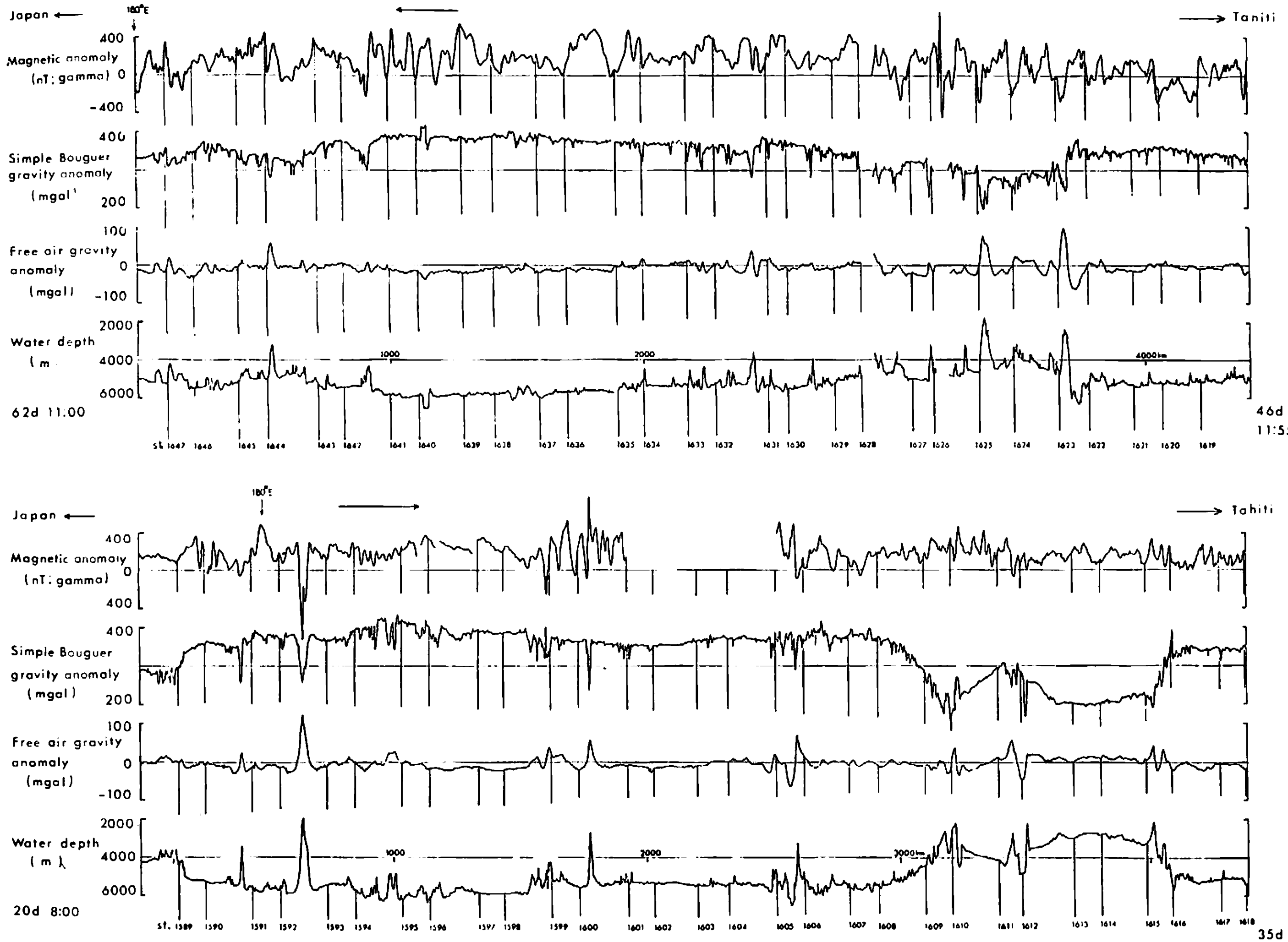

Fig. II-1 Compiled profiles of magnetic anomaly, Bouguer gravity anomaly, free air gravity anomaly, and bathymetry (from the top to the bottom in each profile) along Line A (lower figure) and Line B (upper figure). Vertical line with number indicates the sampling and photographing stations.

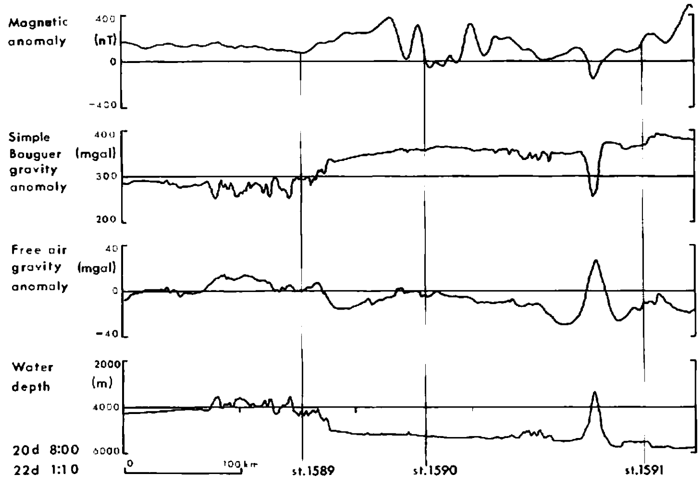

(1)

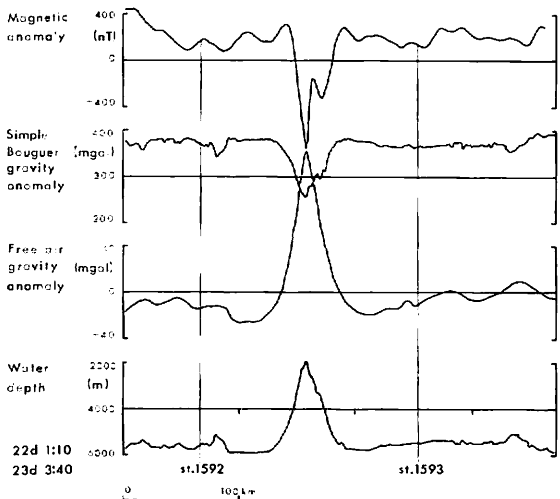

(2)

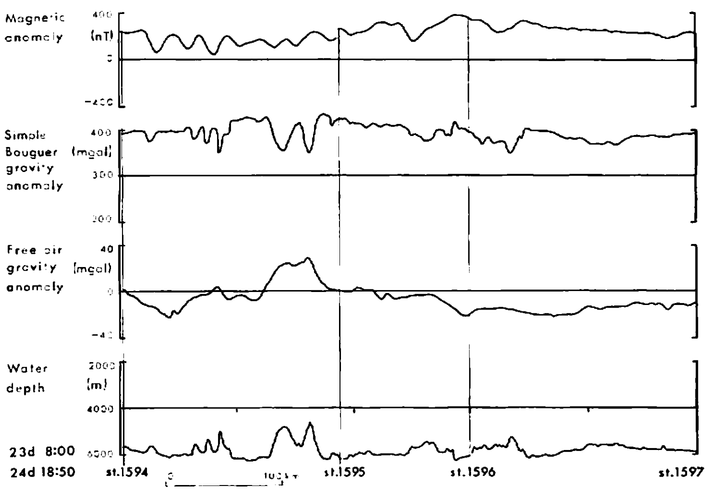

(3)

Fig. II-2 Detailed profiles of geophysical data every intervals of sampling stations (1–18). Arrangement of the data is the same as Fig. II-1.

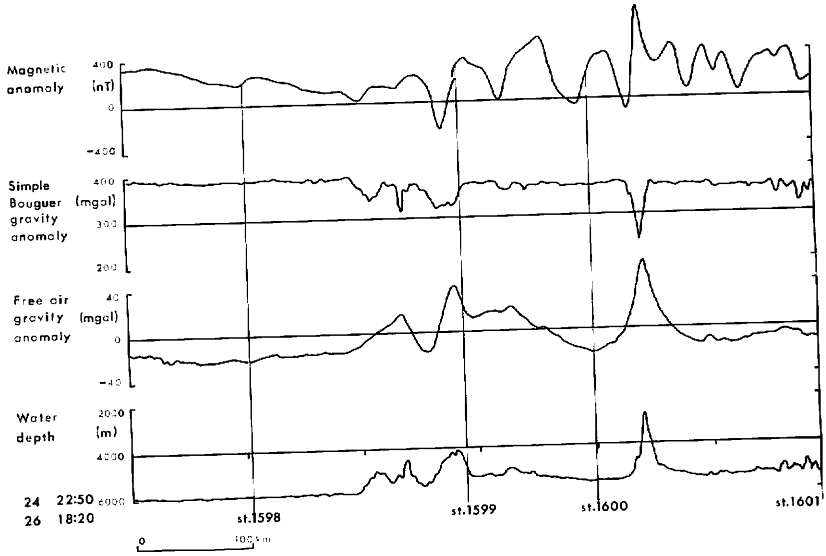

Magnetic anomaly (nT)
400
0
-400
Simple Bouguer gravity anomaly (mgal)
400
300
200
Free air gravity anomaly (mgal)
40
0
-40
Water depth (m)
2000
4000
6000
24 22:50
26 18:20
st.1598
st.1599
st.1600
st.1601
0
100 km

(4)

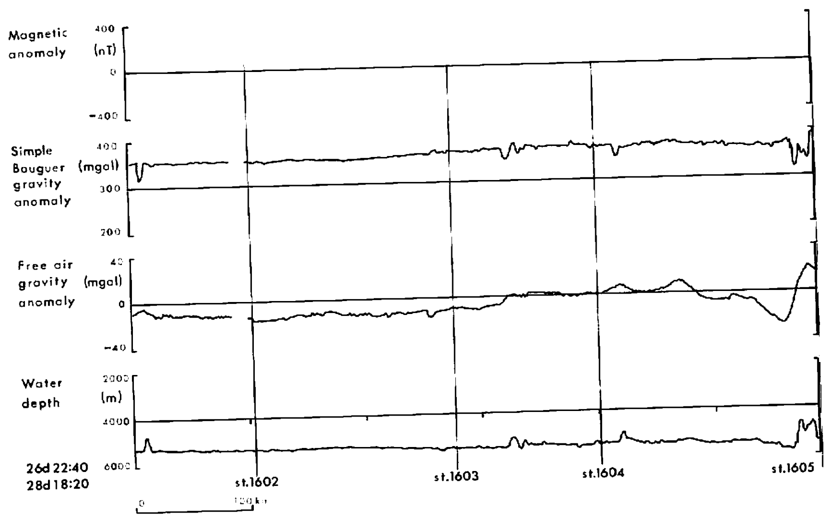

Magnetic anomaly (nT)
400
0
-400
Simple Bouguer gravity anomaly (mgal)
400
300
200
Free air gravity anomaly (mgal)
40
0
-40
Water depth (m)
2000
4000
6000
26d 22:40
28d 18:20
st.1602
st.1603
st.1604
st.1605
0
100 km

(5)

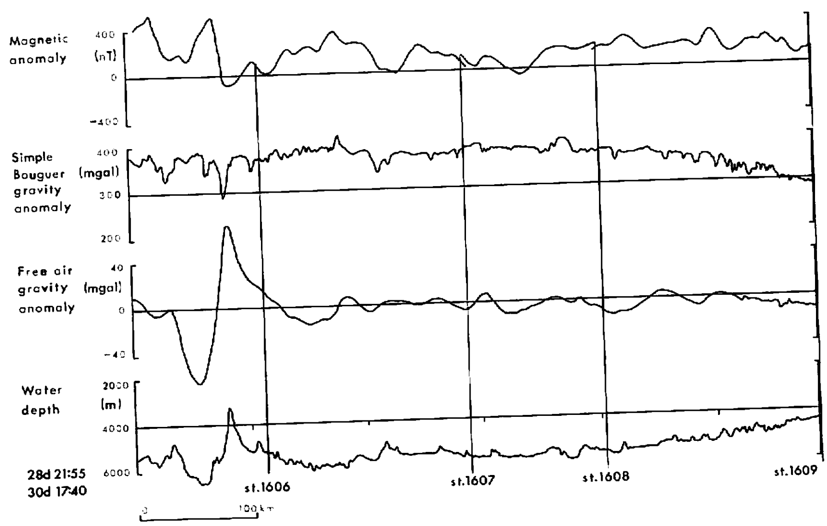

Magnetic anomaly (nT)
400
0
-400
Simple Bouguer gravity anomaly (mgal)
400
300
200
Free air gravity anomaly (mgal)
40
0
-40
Water depth (m)
2000
4000
6000
28d 21:55
30d 17:40
st.1606
st.1607
st.1608
st.1609
0
100 km

(6)

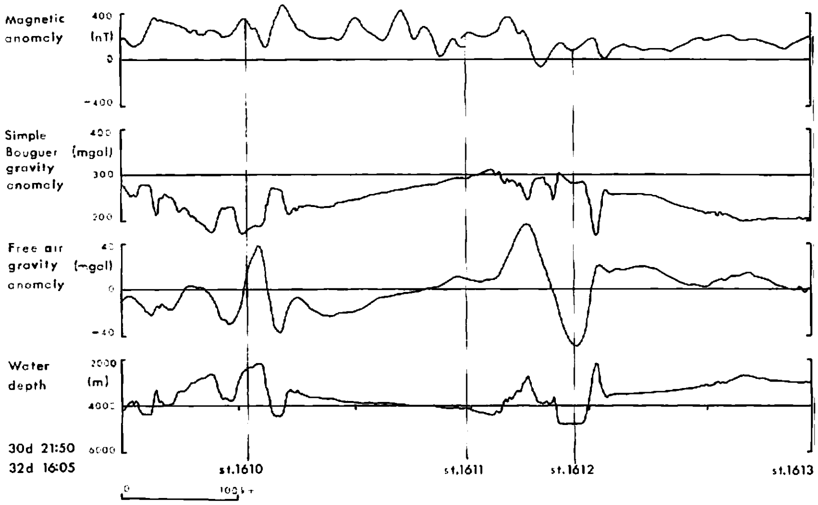
Magnetic anomaly
400
(nT)
0
-400
Simple Bouguer gravity anomaly
400
(mgal)
300
200
Free air gravity anomaly
40
(mgal)
0
-40
Water depth
2000
(m)
4000
6000
30d 21:50
32d 16:05
st.1610
st.1611
st.1612
st.1613

(7)

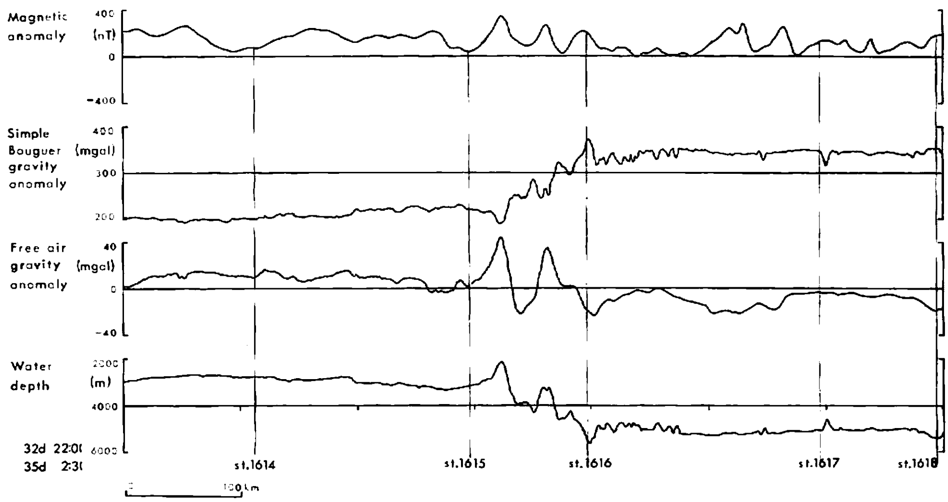
Magnetic anomaly
400
(nT)
0
-400
Simple Bouguer gravity anomaly
400
(mgal)
300
200
Free air gravity anomaly
40
(mgal)
0
-40
Water depth
2000
(m)
4000
6000
st.1614
st.1615
st.1616
st.1617
100km

(8)

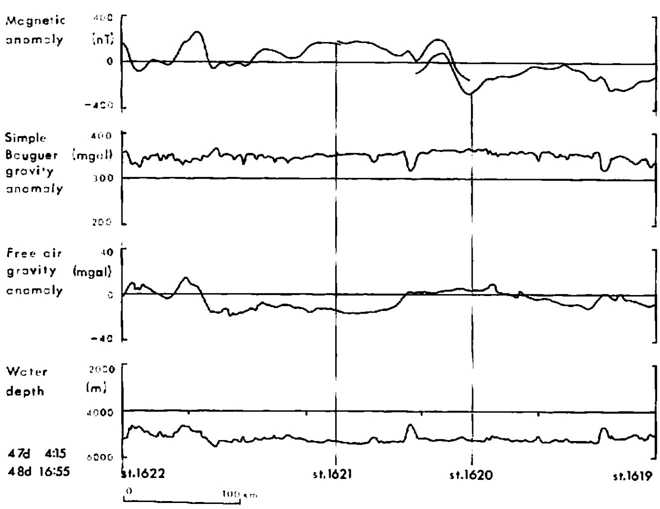
Magnetic anomaly
400
(nT)
0
-400
Simple Bouguer gravity anomaly
400
(mgal)
300
200
Free air gravity anomaly
40
(mgal)
0
-40
Water depth
2000
(m)
4000
6000
47d 4:15
48d 16:55
st.1622
st.1621
st.1620
st.1619
0

(9)

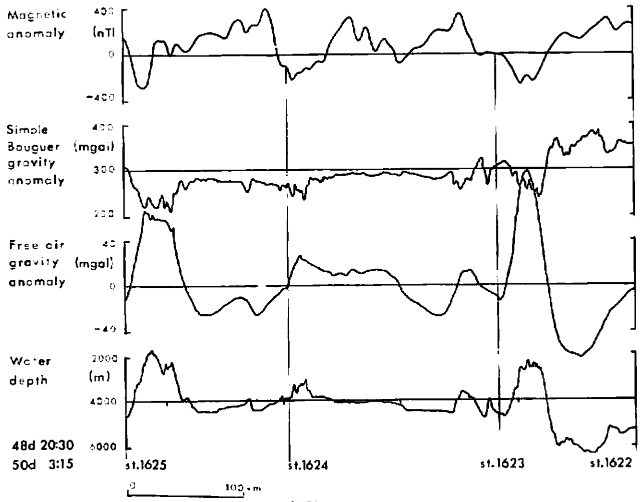

Magnetic anomaly
400
(nT)
0
-400
Simple Bouguer gravity anomaly
400
(mgal)
300
200
Free air gravity anomaly
40
(mgal)
0
-40
Water depth
2000
(m)
4000
6000
48d 20:30
50d 3:15
st.1625
st.1624
st.1623
st.1622
0
100 km

(10)

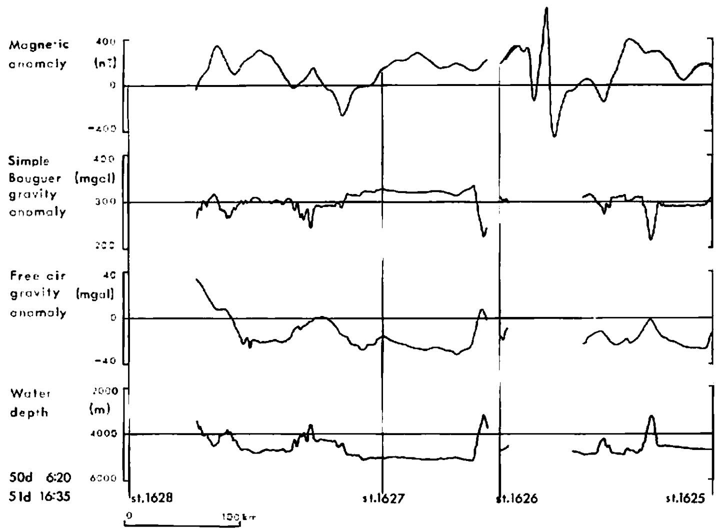

Magnetic anomaly
400
(nT)
0
-400
Simple Bouguer gravity anomaly
400
(mgal)
300
200
Free air gravity anomaly
40
(mgal)
0
-40
Water depth
2000
(m)
4000
6000
50d 6:20
51d 16:35
st.1628
st.1627
st.1626
st.1625
0
100 km

(11)

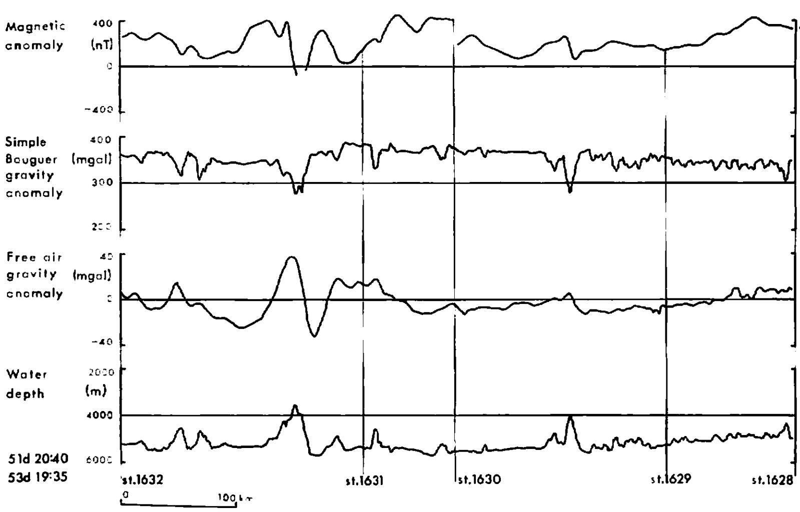

Magnetic anomaly
400
(nT)
0
-400
Simple Bouguer gravity anomaly
400
(mgal)
300
200
Free air gravity anomaly
40
(mgal)
0
-40
Water depth
2000
(m)
4000
6000
51d 20:40
53d 19:35
st.1632
st.1631
st.1630
st.1629
st.1628
0
100 km

(12)

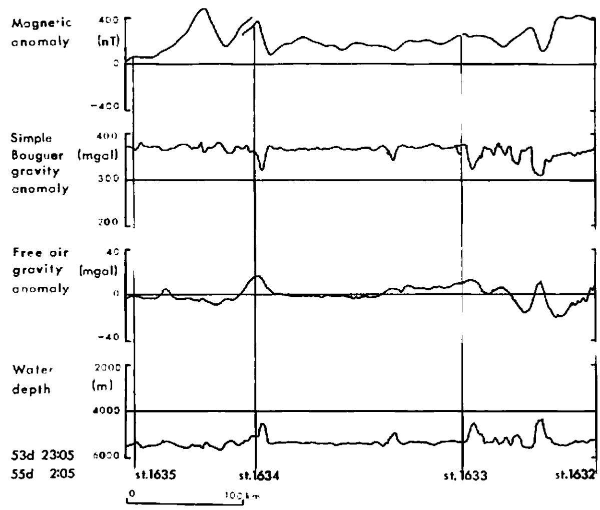
Magnetic anomaly
(nT)
Simple Bouguer gravity anomaly
(mgal)
Free air gravity anomaly
(mgal)
Water depth
(m)
53d 23:05
55d 2:05
st.1635
st.1634
st.1633
st.1632

(13)

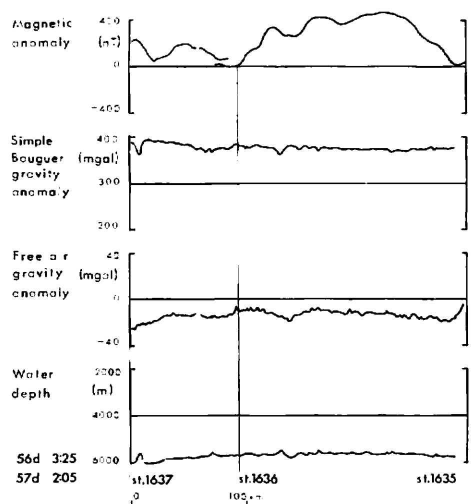
Magnetic anomaly
Simple Bouguer gravity anomaly
(mgal)
Water depth
(m)
56d 3:25
57d 2:05
st.1637
st.1636
st.1635

(14)

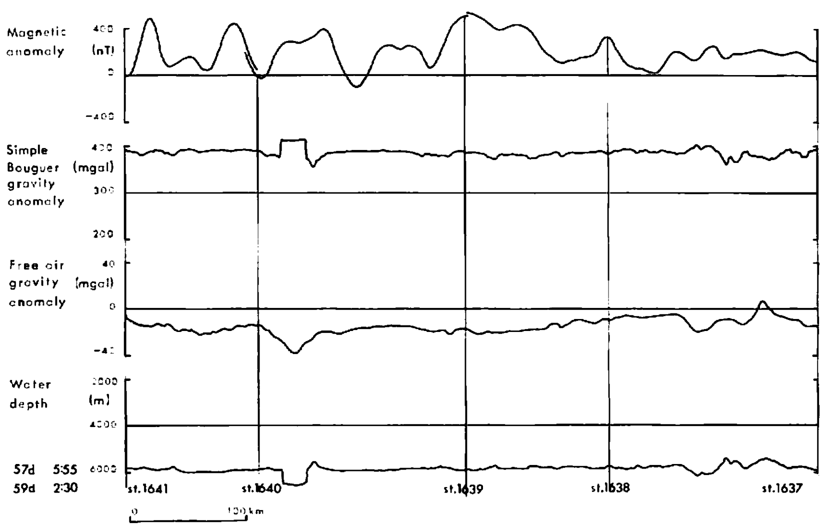
Magnetic anomaly
(nT)
Simple Bouguer gravity anomaly
(mgal)
Free air gravity anomaly
(mgal)
Water depth
(m)
57d 5:55
59d 2:30
st.1641
st.1640
st.1639
st.1638
st.1637

(15)

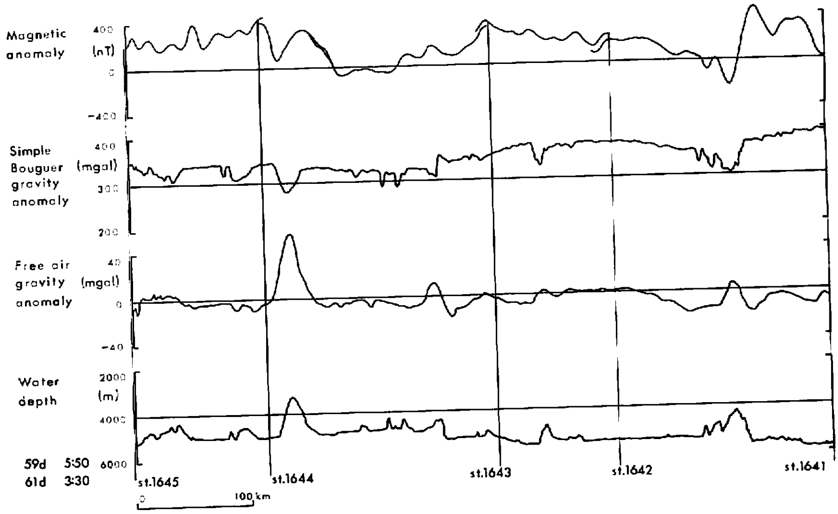

Magnetic anomaly
(nT)
400
0
-400
Simple Bouguer gravity anomaly
(mgal)
400
300
200
Free air gravity anomaly
(mgal)
40
0
-40
Water depth
(m)
2000
4000
6000
59d 5:50
61d 3:30
st.1645
st.1644
st.1643
st.1642
st.1641
0
100 km

(16)

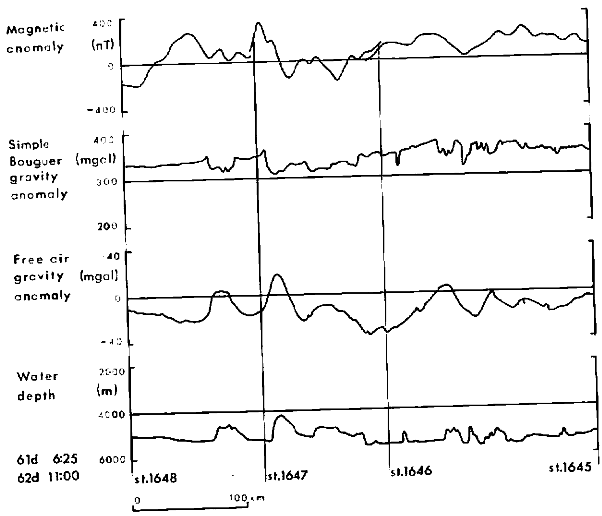

Magnetic anomaly
(nT)
400
0
-400
Simple Bouguer gravity anomaly
(mgal)
400
300
200
Free air gravity anomaly
(mgal)
40
0
-40
Water depth
(m)
2000
4000
6000
61d 6:25
62d 11:00
st.1648
st.1647
st.1646
st.1645
0
100 km

(17)

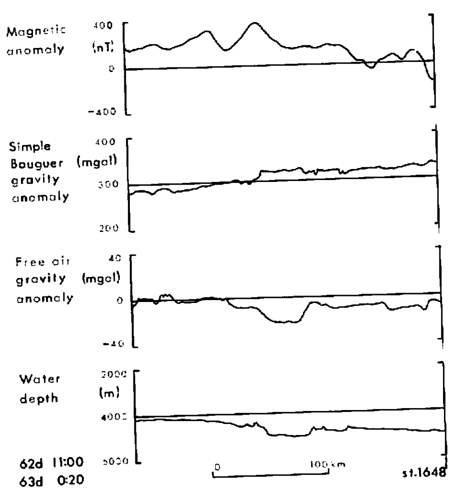

Magnetic anomaly
(nT)
400
0
-400
Simple Bouguer gravity anomaly
(mgal)
400
300
200
Free air gravity anomaly
(mgal)
40
0
-40
Water depth
(m)
2000
4000
6000
62d 11:00
63d 0:20
0
100 km
st.1648

(18)

Table II-1 Gravity data at Tahiti by Woldon Gravitymeter.

Day	Place of measurement	Reading		average	IGSN value*
42 d	Ship side at Papeete Port	1013.6	1015.2	1014.4	978699.6 mgal
42	Hotel Tahiti	989.8		989.8	978696.83
42	Tahiti Air	983.9	984.9	984.4	978696.58
42	ORSTOM	300.8		300.8	

*H. G. BARSCZUS's personal communication.

Table II-2 Drift of gravity value in Sea Air Gravitymeter.

Day	Base reading	Calculated gravity value	IGSN value (in Tahiti*)	Drift
12 d	10699.4	979788.9 mgal	979788.9 mgal	0.0 mgal
38	9615.7	978706.07	978699.6*	6.47
45	9617.5	978707.87	978699.6	8.27
71	10712.4	979801.89	979788.9	12.99

*Personal communication by H. G. BARSCZUS.

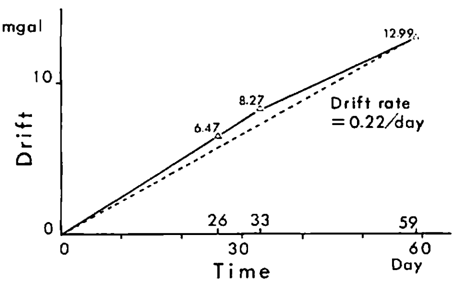

Fig. II-3 Plotted data of gravity meter's drift. Vertical axis is drift (mgal) and horizontal axis is time (day). Drifting rate is calculated to be 0.22/day and it was linear during this cruise.

Gravity data

Gravity data obtained on board were connected with base station at Funabashi Port in Japan and at Papeete in Tahiti. On-shore gravity values in Tahiti measured with Woldon Gravity Meter is shown in Table II-1. Calculated gravity at the ship side at Papeete Port was 978699.6 mgal. Base reading value of the onboard gravity meter changed from 10699.4 to 10712.4 (at Funabashi Port) through 9615.7 (at Papeete Port). The results of calculation of the drift are shown in Table II-2 and Fig. II-3. The drift rate was calculated to be 0.22 mgal/day and the drift was linear during the cruise.

There are several large scale free air gravity anomalies near sea mountains, and the anomalies of 50 to 100 mgal on the seamounts decrease to -20 to -30 mgal at their foot. Bouguer gravity anomaly at the center of the Manihiki Plateau is as high as 300 mgal, whereas it is lowered to 200 mgal around the center of the Plateau. We can recognize a distribution pattern of free air gravity anomaly in the two areas that the value become larger with increasing water depth; associated with change of water depth from 3500 to 4300 m, the value changes from -20 to $+20$ mgal (between Sts. 1610 and 1612, and between Sts. 1612 and 1613). This is interpreted to be caused by thick accumulation of sediments. Abyssal basin usually shows the anomaly of -10 to -20 mgal.

Acknowledgment

We thank Dr. Hans G. BARSCZUS, ORSTOM Center of Papeete, who provided his

unpublished data of gravity in Tahiti stations to us.

References

LARSON, R. L. (1976) Late Jurassic and early Cretaceous evolution of the western Central Pacific Ocean. *Jour. Geomag. Geoelectr.*, vol. 28, p. 219–236.

————, SMITH, S. M., and CHASE, C. G. (1972) Magnetic lineations of early Cretaceous age in the western equatorial Pacific Ocean. *Earth Planet. Sci. Lett.*, vol. 15, p. 315–319.

OEWRIG, J. L. and KROENKE, L. W. (1980) Tectonics of the eastern Central Pacific Basin. *Mar. Geol.*, vol. 34, p. 29–43.

ROSENDAHL, B. R. (1975) Geological and geophysical studies of the Canton Trough region. *Jour. Geophys. Res.*, vol. 80, p. 2565–2574.

TAMAKI, K., JOSHIMA, M., and LARSON, R. L. (1979) Remanent early Cretaceous spreading center in the Central Pacific Basin. *Jour. Geophys. Res.*, vol. 84, p. 4501–4510.